

# Journal of Materials Chemistry C

Accepted Manuscript



This is an *Accepted Manuscript*, which has been through the Royal Society of Chemistry peer review process and has been accepted for publication.

*Accepted Manuscripts* are published online shortly after acceptance, before technical editing, formatting and proof reading. Using this free service, authors can make their results available to the community, in citable form, before we publish the edited article. We will replace this *Accepted Manuscript* with the edited and formatted *Advance Article* as soon as it is available.

You can find more information about *Accepted Manuscripts* in the [Information for Authors](#).

Please note that technical editing may introduce minor changes to the text and/or graphics, which may alter content. The journal's standard [Terms & Conditions](#) and the [Ethical guidelines](#) still apply. In no event shall the Royal Society of Chemistry be held responsible for any errors or omissions in this *Accepted Manuscript* or any consequences arising from the use of any information it contains.

# Fluorinated 9,9'-bianthracene Derivatives with Twisted Intramolecular Charge Transfer Excited States as Blue Host Materials for High-Performance Fluorescent Electroluminescence†

Yue Yu,<sup>a</sup> Zhaoxin Wu,<sup>\*a</sup> Zhanfeng Li,<sup>a</sup> Bo Jiao,<sup>a</sup> Lin Ma,<sup>a</sup> Guijiang Zhou,<sup>\*b</sup> Wai Yu,<sup>c</sup> S. K. So<sup>\*c</sup> and Xun Hou<sup>a</sup>

---

<sup>a</sup>Key Laboratory of Photonics Technology for Information, Department of Electronic Science and Technology, School of Electronic and Information Engineering, Xi'an Jiaotong University, Xi'an 710049, People's Republic of China. E-mail: zhaoxinwu@mail.xjtu.edu.cn; Fax: (+86) 029-82664867

<sup>b</sup>Department of Chemistry, School of Science, Xi'an Jiaotong University, Xi'an 710049, People's Republic of China. E-mail: zhougj@mail.xjtu.edu.cn

<sup>c</sup>Department of Physics and Institute of Advanced Materials, Hong Kong Baptist University, Hong Kong, 999077 People's Republic of China. E-mail: skso@hkbu.edu.hk

## Abstract

The authors report the electroluminescent (EL) performance of a series of fluorinated 9,9'-bianthracene derivatives (BAnFs) to serve as host materials. With the different position of F substitution pattern, the EL performances are strongly affected. In particular, 10,10'-bis(4-fluorophenyl)-9,9'-bianthracene (BAn-(4)-F) works as an excellent fluorescent host for *N,N*-diphenylamino phenyl vinyl biphenyl (DPAVBi) and 10-(2-benzothiazolyl)-1,1,7,7-tetramethyl-2,3,6,7-tetrahydro-1*H*,5*H*,11*H*-benzo[*l*]pyrano(6,7-*ij*)quinolizin-11-one (C545T) dopants to get high-performance organic light-emitting diodes (OLEDs) with excellent external quantum efficiencies (EQEs) of 5.43% and 5.20%, respectively. We demonstrate that, the improved EQEs are due to the enhanced occurrence of singlet excitons in BAn-(4)-F-based EL devices. The BAn-(4)-F host molecule with particular twisted intramolecular charge transfer (TICT) excited state, which is a charge-transfer (CT) intersystem crossing mechanism, realizes the transition from triplet CT-state to singlet CT-state. At the dopant site, the available singlet excitons formed via Förster energy transfer from host BAn-(4)-F to dopant are greatly increased. It is concluded that the BAn-(4)-F host based on 9,9'-bianthracene can significantly enhance the singlet generation fraction in EL device.

## 1. Introduction

Organic light-emitting diode (OLED) based display and solid-state lighting technologies are a promising alternative to traditional inorganic light-emitting diode (LED) based display and solid-state lighting technologies because they can be brighter, more adaptable, longer-lived, and more energy efficient.<sup>1-4</sup> For full-color display and white lighting, it is essential to have the three primary colors, red, green, and blue. However, the progress in highly efficient blue OLEDs is far behind counterparts of green/red OLEDs due to the difficulty to develop blue-emitting materials with high efficiency, color purity, efficient transport, and long operation time, thus it is necessary to improve their performance for display or lighting applications. For the development of fluorescence emitting compounds for OLEDs, blue emitting compounds are particularly worth studying because long practical lifetimes are more difficult to achieve for blue phosphorescent devices than fluorescence ones. It is well known that a dopant/host doped emitter system can significantly avoid concentration quenching of fluorescence and improve device performance in terms of electroluminescent (EL) efficiency and emissive color, as well as operational lifetime.<sup>5</sup> Various blue host materials have been reported to date, which include anthracene, fluorene, styrylarylene, pyrene, quinoline and triphenylene derivatives.<sup>6-11</sup> Among these, the anthracene-cored fluorescent emitters with intrinsic wide-energy band gap, high fluorescence quantum yield, and high thermal stability as well as nondispersive ambipolar carrier transporting properties, have attracted considerable interest in blue OLEDs.<sup>6</sup>

As we know, the relative energetics and rates of formation for singlet versus triplet excited states can have a significant impact on device efficiency, fluorescence efficiency within OLEDs is directly related to the fraction of singlet exciton states produced because only those states can fluoresce to emit light. This singlet state fraction can be increased above the statistically expected 25%<sup>12</sup> if triplet states undergo rapid intersystem crossing (ISC) to become singlet states.<sup>13</sup> In order to

improve the efficiency of fluorescent OLEDs, Baldo, Adachi and their colleagues used charge transfer (CT) state to form radiative exciton or used radiative CT exciton immediately to break the limit of singlet generation fraction 25%.<sup>14</sup>

9,9'-Bianthracene (BA) is the most thoroughly investigated member of the family of symmetrical, nonpolar biaryls which undergo a symmetry breaking with formation of a highly polar intramolecular CT state in the excited state and especially in polar solvents.<sup>15,16</sup> Both experimental data and quantum-chemical calculations indicate that the ground-state conformation corresponds to a twist angle  $\theta \approx 90^\circ$ , due to the strongly repulsive interaction of the hydrogen atoms at the 1,1'- and 8,8'-position.<sup>17</sup> The two anthracene groups are electronically decoupled because of orthogonal structure in the ground state, while they exhibit a strong electronic interaction with the relaxation of geometric structure in the excited state.<sup>18</sup> Peng Zhang, etc, demonstrated the ability of twisted intramolecular charge transfer (TICT) state to enhance the fraction of singlet excitons in a nondoped EL device used a fluorescent emitter that is based on the BA moiety. The BA-cored fluorescence emitters with particular TICT characteristics realize the electron-hole recombination via intramolecular conversion from CT excitons (immediate precursor) to radiative singlet exciton (final state).<sup>19</sup>

Fluorination has been used in the past decade as a route to induce stability and electron transport or ambipolar transport in organics by lowering the energy levels in the small molecules or polymers, especially for OLEDs.<sup>20-24</sup> Moreover, the C-H...F interactions, similar to a hydrogen bond, play an important role in the solid state organization of fluorine compounds bearing both C-F and C-H bonds, originating a typical  $\pi$ -stack arrangement which enhances the charge carrier mobility.<sup>22,23,25,26</sup>

Herein, we have synthesized a series of fluorinated BA derivatives (BAnFs). We recently reported these BAnFs to serve as deep-blue dopants in organic EL devices.<sup>24d</sup> In this paper, we studied the performances of these BAnFs as hosts. Compared with other BAnFs, 10,10'-bis(4-fluorophenyl)-9,9'-bianthracene (BAn-(4)-F) showed the most excellent performance. For BAn-(4)-F-based EL device, the external quantum efficiency (EQE) is more than 5%, and the efficiency roll-off is negligible due to the

excellent ambipolar transport of BAn-(4)-F induced by appropriate fluorination. Further, we demonstrated doped devices used BAn-(4)-F as hosts doubled the fraction of singlet excitons. We have found that there is a TICT-state of host BAn-(4)-F, which is more likely to have a higher ISC rate to enhance the singlet generation fraction in EL device significantly.

## 2. Results and discussion

The chemical structures of BAnFs in this study are shown in Fig. 1. Physical properties of the compounds are summarized in Table S1 (see ESI†). The details of synthesis, theoretical computation, thermal properties, photophysical properties and electrochemical properties are described in our previous work.<sup>24d</sup>

### 2.1 Photophysical and excited state properties

As shown in Fig. S1 (see ESI†), taken BAn-(4)-F for example, the PL spectra of BAn-(4)-F exhibit red-shift of 40 nm when the solvent polarity is raised from 2.4 (toluene) to 5.8 (acetonitrile). This phenomenon is consistent with a variety of the excited state from the locally excited state (LE-state) to an excited state with the strong CT character involving the TICT mechanism of BA core.<sup>27</sup> Additionally, the fluorescence blueshift observed for BAn-(4)-F in the film as compared to that in solution indicates reduced conjugation, which is caused by the fragment twisting. This implies that BAn-(4)-F based on BA in the excited state exhibit intramolecular twisting toward planarization.

### 2.2 Morphological properties

The density functional theory (DFT) calculation results indicate that BAnFs have extremely twisted geometry configurations, which can prevent intramolecular extending of  $\pi$ -electron and suppress intermolecular interactions, conjugation, and molecular recrystallization. All BAnFs show considerable thermal stability, which have high  $T_g$  values above 150°C. The high stability of the amorphous glass state of these compounds is attributed to the non-planarity of their molecular structures, demonstrating that the perpendicular-type BA core improves the thermal stability

efficiently. Therefore, these chromophores are thermally stable and suitable for vapor deposition in OLEDs fabrication. Fig. 2 shows the surface morphology of vacuum-deposited 3 wt% DPAVBi-doped films (ca. 50nm) on indium tin oxide (ITO) by atomic force microscopy (AFM). The doping films of BAn-(2)-F, BAn-(3)-F, BAn-(4)-F, BAn-(2,4)-F and BAn-(3,4,5)-F have root-mean-square of surface roughness ( $R_{RMS}$ ) of 2.24, 2.10, 2.08, 2.32 and 2.40 nm, respectively, and show pin-free and smooth surface morphology. For a direct comparison, we used 4,4'-bis(2,2-diphenylvinyl)-1,1'-bibenyl (DPVBi) and 2-*tert*-butyl-9,10-di(2-naphthyl)anthracene (TBADN) as control materials. The surface morphology of DPVBi and TBADN doping films were also shown in Fig. 2 with the  $R_{RMS}$  of 4.10 and 2.01 nm. The AFM investigations indicate that both these vacuum-deposited films of BAnFs and TBADN have good morphological properties compared to that of DPVBi.

### 2.3 Carrier-transport properties

To investigate the carrier-transport properties of BAnFs, electron-only and hole-only devices with structure of ITO/LiF (1 nm)/1,3,5-tris(1-phenyl-1*H*-benzimidazol-2-yl)benzene (TPBi) (10 nm)/BAnF or 4,4'-bis(*N*-carbazolyl)biphenyl (CBP) (80 nm)/TPBi (10 nm)/LiF (1 nm)/Al (100 nm) and ITO/molybdenum trioxide ( $\text{MoO}_3$ ) (3 nm)/4,4'-bis[*N*-(1-naphthyl)-*N*-phenyl-amino]biphenyl (NPB) (10 nm)/BAnF or CBP (80 nm)/NPB (10 nm)/ $\text{MoO}_3$  (3 nm)/Al (100 nm), respectively, were prepared. For a direct comparison, we used the well known ambipolar conductive CBP as a comparison.<sup>28</sup> Their current–voltage properties of these devices are shown in Fig. 3, on one hand, for the electron-only devices, it can be seen that the current density at a given applied voltage exhibits BAn-(4)-F > BAn-(3)-F  $\approx$  BAn-(2)-F > BAn-(2,4)-F > BAn-(3,4,5)-F > CBP, suggesting their electron mobility decreased in turn. Obviously, the BAnFs exhibit much higher electron mobility than CBP, especially for BAn-(4)-F. On the other hand, for the hole-only devices, the current density at a given applied voltage shows CBP  $\approx$  BAn-(2)-F > BAn-(3)-F  $\approx$

BAn-(4)-F > BAn-(2,4)-F > BAn-(3,4,5)-F, suggesting their hole mobility decreased in turn, it is seemed that BAn-(2)-F and CBP have the same performance on hole mobility, BAn-(3)-F and BAn-(4)-F show slightly lower hole mobility than CBP, BAn-(2,4)-F and BAn-(3,4,5)-F exhibit poorer performances. This is attributed to the incorporation of much more electronegative F groups in the molecule, which lowered significantly the hole mobility. As we all know, the hole mobility of CBP is much higher than its electron mobility, therefore, BAnFs are expected to have more balanced ambipolar conductive property. The carrier mobilities of the BAn-(4)-F film were further characterized by the time-of-flight (TOF) transient-photocurrent technique.<sup>29</sup> The carrier mobility ( $\mu$ ) was calculated from the values of the transit time ( $T_t$ ), the sample thickness ( $D$ ) and the applied voltage ( $V$ ) by using the following equation:  $\mu = D^2/(VT_t)$ . For comparison, we also carry out experiment on hole mobility of NPB. As shown in Fig. 3c, BAn-(4)-F has extremely balanced ambipolar conductive property for its very electron mobility is very close to hole mobility. BAn-(4)-F displays high electron mobility ( $\sim 10^{-3} \text{ cm}^2 \text{ V}^{-1} \text{ s}^{-1}$ ) at an electric field of  $4 \times 10^5 \text{ V cm}^{-1}$ , which is comparable to the highest reported electron mobility,<sup>30</sup> and is about three orders of magnitude higher than that of the typical ETL material tris(8-hydroxyquinoline)aluminum ( $\text{Alq}_3$ ),  $\sim 10^{-6} \text{ cm}^2 \text{ V}^{-1} \text{ s}^{-1}$  (@  $0.8 \times 10^6 \text{ V cm}^{-1}$ ).<sup>31</sup> BAn-(4)-F also exhibits high hole mobility that is close to the electron mobility. The mobility exceeds that of a typical hole transport material *N,N'*-bis(naphthalen-1-yl)-*N,N'*-bis(phenyl)benzidine (NPB) by one order of magnitude.<sup>32</sup> BAnFs have wide optical energy gaps of 3.04 to 3.08 eV. Accordingly, BAnFs could be expected to be suitable candidates for host materials for highly efficient fluorescent OLEDs.

## 2.4 Electroluminescent properties

We have reported the EL properties of BAnFs as deep-blue dopants.<sup>24d</sup> In order to explore OLEDs characteristics of BAnFs, we have fabricated non-doped blue devices (for details, see ESI†). To study the EL performance of BAnFs as host materials on the

basis of BAnFs' wide band gaps, balanced ambipolar carrier transporting abilities, and film forming abilities, doping devices have been fabricated and evaluated by using the well known *N,N*-diphenylamino phenyl vinyl biphenyl (DPAVBi) as the blue fluorescent dopant. As shown in Fig. 4, the DPAVBi-doped devices (1-5A) were fabricated with the following configuration: ITO/poly(3,4-ethylenedioxythiophene) : poly(styrenesulfonate) (PEDOT : PSS) (30 nm)/NPB (30 nm)/4,4',4''-tris(carbazol-9-yl)-triphenylamine (TcTa) (10 nm)/blue emitting layer (EML) (30 nm)/TPBi (40 nm)/CsCO<sub>3</sub> (3 nm)/Al (100 nm). PEDOT : PSS was used as hole injection layer (HIL), NPB was used as hole transporting layer (HTL), TcTa was used as exciton blocking layer, TPBi was used as electron transporting layer (ETL) and exciton blocking layer, and CsCO<sub>3</sub> was used as electron injection layer (EIL), respectively. DPAVBi was co-evaporated with each host to give the optimal doping concentration of 3 wt% in EML. Fig. 5b shows the normalized EL spectra for the DPAVBi-doped devices. All of the blue EL spectra of DPAVBi-doped devices show bright blue emissions with vibronic peaks around 470 and 490 nm, characteristic of the emissions from the DPAVBi dopant, while the film PL peak of the host material itself is at a shorter wave length as shown in Fig. 5a. This result indicates that the light emission originates from the DPAVBi dopant, rather than from the blue host materials BAnFs. Fig. 6 and 7 exhibits the current density–voltage–luminance–efficiency (*J–V–L–η*) characteristics of the DPAVBi-doped BAnF devices. The key device performance parameters and EL emission characteristics are summarized in Table 1. These DPAVBi-doped BAnF devices display low turn-on voltages (at a luminance of 1 cd m<sup>-2</sup>) no greater than 4.4 V. We note that good to excellent performance of blue OLEDs can be achieved by using BAnFs as the hosts. The current efficiency and power efficiency of these devices are in the range 7.05–9.64 cd A<sup>-1</sup> and 4.46–6.77 lm W<sup>-1</sup>, respectively. The high EL efficiencies of the DPAVBi-doped BAnF devices can be attributed mainly to good injection of carrier charges and good confinement of both carriers and excitons within the EML. Since the HOMO levels of the hosts (from –5.68 to –5.77 eV) and TcTa (–5.7 eV) are almost same, similarly the LUMO levels of the hosts (from –2.63 to –2.69 eV) and TPBi (–2.7 eV) are almost same too, the

barriers for hole injection from the TcTa layer to the emissive layer and electron injection from the TPBi layer to the emissive layer can be neglected. Thus, the carrier charges will easily transport into the host layers and recombine within this layer. Meanwhile, carriers and excitons are well confined within the EML due to the higher LUMO levels of TcTa ( $-2.4$  eV) and the lower HOMO levels of TPBi ( $-6.2$  eV). Notably, the device with BAn-(4)-F as the host achieves the best EL performance, with a maximum luminance of  $28667$   $\text{cd m}^{-2}$ , a maximum EQE as high as  $5.43\%$ , a maximum current efficiency of  $9.64$   $\text{cd A}^{-1}$ , a maximum power efficiency of  $6.77$   $\text{lm W}^{-1}$  and blue emission at Commission Internationale de l'Éclairage (CIE) coordinates of (0.15, 0.27). The performance of the BAn-(4)-F device was outstanding compared to previously reported results for DPAVBi-doped fluorescence blue-light-emitting OLEDs.<sup>33</sup> It's worth noting that the efficiency roll-off of the BAn-(4)-F-based device is negligible. It shows an EQE over  $97.7\%$  of maximum EQE at an illumination-relevant luminance of  $1\ 000$   $\text{cd m}^{-2}$ , in comparison with  $97.5\%$  for the BAn-(2)-F-based device,  $93.4\%$  for the BAn-(3)-F-based device,  $94.8\%$  for the BAn-(2,4)-F-based device, and  $92.4\%$  for the BAn-(3,4,5)-F-based device, it still maintained  $92\%$  of maximum EQE at an illumination-relevant luminance of  $1\ 0000$   $\text{cd m}^{-2}$ , in comparison with  $79.5\%$  for the BAn-(2)-F-based device,  $80.5\%$  for the BAn-(3)-F-based device,  $82.6\%$  for the BAn-(2,4)-F-based device, and  $73.2\%$  for the BAn-(3,4,5)-F-based device. The excellent ambipolar transport of BAn-(4)-F induced by appropriate fluorination contributes mainly to the low roll-off of the BAn-(4)-F-based device (see Fig. 3). Meanwhile, the HOMO and LUMO energy levels of BAn-(4)-F are matched well with the neighboring TcTa HTL and TPBi ETL, thus leading to good injection of carrier charges and good confinement of both carriers and excitons within the EML. The high efficiency and low efficiency roll-off of the BAn-(4)-F-based device is attributed to a better balance of electron- and hole-transport properties.

To further investigate the EL properties of the BAn-(4)-F host, two groups of devices using DPAVBi as the blue fluorescent dopant and 10-(2-benzothiazolyl)-1,1,7,7-tetramethyl-2,3,6,7-tetrahydro-1*H*,5*H*,11*H*-benzo[*l*]pyr

6,7,8-quinolin-11-one (C545T) as the green fluorescent dopant, respectively, were fabricated. The configuration of these comparative devices are as below:

Device 1B: ITO/MoO<sub>3</sub> (3 nm)/NPB (30nm)/TcTa (10nm)/BAn-(4)-F: DPAVBi (3 wt%) (30nm)/TPBi (40nm)/LiF (1nm)/Al (100 nm)

Device 2B: ITO/MoO<sub>3</sub> (3 nm)/NPB (30nm)/TcTa (10nm)/TBADN: DPAVBi (3 wt%) (30nm)/TPBi (40nm)/LiF (1nm)/Al (100 nm)

Device 1C: ITO/MoO<sub>3</sub> (3 nm)/NPB (40nm)/BAn-(4)-F: C545T (2 wt%) (30nm)/TPBi (40nm)/LiF (1nm)/Al (100 nm)

Device 2C: ITO/MoO<sub>3</sub> (3 nm)/NPB (60nm)/tris-(8-hydroxyquinoline)aluminum (Alq<sub>3</sub>): C545T (2 wt%) (30nm)/TPBi (30nm)/LiF (1nm)/Al (100 nm)

BAn-(4)-F was used as host to fabricate Device 1B and 1C. Device 2B and 2C, used TBADN and Alq<sub>3</sub> as host, respectively, were fabricated for the control experiments. Fig. 8 shows the normalized EL spectra for the four devices. The EL spectra of Device 1B and 2B show blue emissions of DPAVBi with the same peaks at 468 and 492 nm (shoulder peak), while the EL spectra of Device 1C and 2C show green emissions of C545T with the peaks at 504 and 524 nm, respectively. This behavior of different EL spectra could originate from the conformational change of the dopant material (C545T) in the excited state in both hosts. The voltage–current density characteristics and the EQE curves of the devices are illustrated in Fig. 9 and the key devices performances are listed in Table 2. There are no distinct differences in the voltage–current density characteristics of both Device 1B, 2B and Device 1C, 2C, which indicates that the variation in charge balance is not the main reason for their different EL performances. Most notably, the EQEs of Device 1B, 2B, 1C and 2C are 5.42, 3.13, 5.20 and 3.52%, respectively. the BAn-(4)-F-based devices (1B, 1C) display higher performances than the control ones (2B, 2C). On the contrary, the absolute photoluminescence quantum yield (PLQY) of BAn-(4)-F: DPAVBi (3 wt%) (0.42) is lower than that of TBADN: DPAVBi (3 wt%) (0.51), and the PLQY of BAn-(4)-F: C545T (2 wt%) (0.48) is lower than that of Alq<sub>3</sub>: C545T (2 wt%) (0.62) in thin film. EQE of the fluorescent OLED is estimated from the equation  $\eta_{\text{EL}} = \alpha \gamma \chi_s \Phi_{\text{PL}}$ , where  $\alpha$  is the light output coupling factor,  $\gamma$  is the probability of carrier

recombination,  $\chi_s$  is the production efficiency of a singlet exciton, and  $\Phi_{\text{PL}}$  is the absolute PLQY of the emitter.<sup>34</sup> Ideally, assuming that  $\chi_s$  of Device 2B is 25.0% and both Device 1B and 2B have the same  $\alpha$  and  $\gamma$ ,  $\chi_s$  of Device 1B is calculated to be 56.6%. On the same assumption,  $\chi_s$  of Device 1C is calculated to be 47.7%. We can come to a conclusion that the BAn-(4)-F host can significantly enhance the  $\chi_s$  in EL devices. Nevertheless, the triplet-triplet annihilation (TTA) does not play a role in achieving high  $\chi_s$ , because the luminance increases linearly with increasing current density at low current injection (from 0.1 to 3 mA/cm<sup>2</sup>) and less than linearly at higher current injection<sup>35</sup>, as shown in Fig. S2 (see ESI†).

As shown in Fig. 10, these are two kinds of mechanism in BAn-(4)-F-based devices: carrier trapping at the dopant sites and Förster energy transfer from host to dopant. The higher-lying dopant HOMO (−5.3 eV) with respect to the host HOMO (−5.7 eV) prompts the DPAVBi molecules to serve as hole-traps, while the C545T molecules may act as good electron-traps according to the large level difference (0.7 eV) between the LUMO of C545T (−3.3 eV) and BAn-(4)-F (−2.6 eV). In the process of carrier trapping, the standard statistical value of the single to triplet ratio is 1:3.<sup>36</sup> Now we mainly focus on Förster energy transfer from host to dopant.

According to Zhang et al.,<sup>19</sup> for BAn-(4)-F-based devices (Device 1B, 1C), there are two channels might bring about the bound electron-hole pair of host molecule. On the one hand, the electron-hole pair localizes at one anthracene plane to form tightly bound LE-state, this process will produce only one singlet exciton (<sup>1</sup>LE) for every three triplet excitons (<sup>3</sup>LE). On the other hand, the electron and hole of a bound electron-hole pair may reside on two anthracene rings of one molecule respectively to form bound perpendicular TICT (p-TICT) state due to the almost perpendicular configuration of two anthracene rings. The p-TICT state that will undergo geometry relaxation of the BA moiety by a slight torsion, results in a mixing state of singlet CT-state (<sup>1</sup>CT-state) and triplet CT-state (<sup>3</sup>CT-state). The twisted nature of the excited-state increases the spin-orbit coupling mediated mixing between the singlet and triplet states, thus a twisted CT state is more likely to have a higher ISC rate than that of a planar LE state.<sup>37</sup> The TICT-state is a spin-orbit, charge-transfer intersystem

crossing mechanism, it is possible for the transition  $^3\text{CT} \rightarrow ^1\text{CT}$  to become allowed due to the energetic closeness between them,<sup>38</sup> especially in the perpendicular orientation between the donor and acceptor, the ISC rate is enhanced.<sup>39</sup> At last,  $^1\text{CT}$ -state and  $^1\text{LE}$  of host may give energy to dopant via Förster energy transfer. The whole process was described in Fig. 10, throughout the process, the singlet state fraction can be increased above the statistically expected 25% because  $^3\text{CT}$  states undergo rapid ISC to become  $^1\text{CT}$  states. If we ignore carrier trapping at the dopant site, Assuming that the proportion of LE-state and CT-state is 1:1 and all of the  $^3\text{CT}$  states turn into  $^1\text{CT}$ , we can estimate about maximum generation rate of singlet state at the dopant site, e.g.,  $0.5 \times 0.25 + 0.5 = 62.5\%$ . In consideration of carrier trapping and other idealized assumption, the result is agreed with experimental values of Device 1B (56.6%) and Device 1C (47.7%). The generation rate of singlet state of Device 1C is lower than Device 1B due to greater carrier trapping of C545T dopant in Device 1C.

### 3. Conclusions

In summary, a series of BAnFs have been successfully used as host materials. By the introduction of F substitution pattern in different position, we have demonstrated that the carrier-transport properties and OLED performances are significantly affected. EL characterization indicates that, as a host material doped with the blue fluorescent dopant DPAVBi, the performance of the BAn-(4)-F-based device is rather excellent, displaying a maximum current efficiency of  $9.64 \text{ cd A}^{-1}$ , a maximum EQE of 5.43% and CIE coordinates of (0.15, 0.27). We have found that there is a twisted CT state of host BAn-(4)-F, which is more likely to have a higher ISC rate for the transition  $^3\text{CT} \rightarrow ^1\text{CT}$ , significantly enhancing the singlet generation fraction in EL device.

## 4. Experimental

### 4.1 General information

The BAnFs were synthesized by following our previously reported work.<sup>24d</sup> General

experimental informations of physical properties of the compounds are described in our previous work.<sup>24d</sup> The absolute PL quantum yields were measured using an integrating sphere excited at 380 nm with an absolute PL quantum yield measurement system (Hamamatsu C11347).

## 4.2 Devices fabrication and testing

OLEDs were fabricated by thermal evaporation onto a cleaned glass substrate precoated with transparent and conductive indium tin oxide (ITO). Prior to organic layer deposition, ITO substrates were exposed to a UV-ozone flux for 10 min, following degreasing in acetone and isopropyl alcohol (IPA). All of the organic materials were purified by temperature-gradient sublimation in a vacuum. The devices were fabricated by conventional vacuum deposition of the organic layers, MoO<sub>3</sub>, LiF, CsCO<sub>3</sub> and Al cathode onto an ITO-coated glass substrate under a base pressure lower than  $1 \times 10^{-3}$  Pa. The thickness of each layer was determined by a quartz thickness monitor. The voltage–current density ( $V$ – $J$ ) and voltage–brightness ( $V$ – $L$ ) as well as the current density–current efficiency ( $J$ – $\eta_c$ ) and current density–power efficiency ( $J$ – $\eta_p$ ) curve characteristics of devices were measured with a Keithley 2602 and Source Meter. All measurements were carried out at room temperature under ambient conditions.

## Acknowledgements

This work was financially supported by Basic Research Program of China (2013CB328705), National Natural Science Foundation of China (Grant Nos. 61275034, 61106123 ), Ph.D. Programs Foundation of Ministry of Education of China (Grant No. 20130201110065) and Fundamental Research Funds for the Central Universities (Grant No. xjj2012087).

## References

- 1 C. W. Tang and S. A. VanSlyke, *Appl. Phys. Lett.*, 1987, **51**, 913.
- 2 L. S. Hung and C. H. Chen, *Mater. Sci. Eng., R*, 2002, **39**, 143.
- 3 S. R. Forrest, *Nature*, 2004, **428**, 911.

- 4 Y. Sun, N. C. Giebink, H. Kanno, B. Ma, M. E. Thompson and S. R. Forrest, *Nature*, 2006, **440**, 908.
- 5 C. W. Tang, S. A. VanSlyke and C. H. Chen, *J. Appl. Phys.*, 1989, **65**, 3610.
- 6 (a) Y. H. Kim, D. C. Shin, S. H. Kim, C. H. Ko, H. S. Yu, Y. S. Chae and S. K. Kwon, *Adv. Mater.*, 2001, **13**, 1690; (b) J. Shi and C. W. Tang, *Appl. phys. lett.*, 2002, **80**, 3201; (c) Y. Kan, L. Wang, L. Duan, Y. Hu, G. Wu and Y. Qiu, *Appl. phys. lett.*, 2004, **84**, 1513; (d) Y. H. Kim, H. C. Jeong, S. H. Kim, K. Y. Yang and S. K. Kwon, *Adv. Funct. Mater.*, 2005, **15**, 1799; (e) P.-T. Shih, C.-Y. Chuang, C.-H. Chien, E.W.-G. Diau and C.-F. Shu, *Adv. Funct. Mater.*, 2007, **17**, 1341; (f) Y. Y. Lyu, J. Kwak, O. Kwon, S. H. Lee, D. Kim, C. Lee and K. Char, *Adv. Mater.*, 2008, **20**, 2720; (g) C. H. Chien, C. K. Chen, F. M. Hsu, C. F. Shu, P. T. Chou and C. H. Lai, *Adv. Funct. Mater.*, 2009, **19**, 560; (h) C. J. Zheng, W. M. Zhao, Z. Q. Wang, D. Huang, J. Ye, X. M. Ou, X. H. Zhang, C. S. Lee and S. T. Lee, *J. Mater. Chem.*, 2010, **20**, 1560; (i) K. H. Lee, J. K. Park, J. H. Seo, S. W. Park, Y. S. Kim, Y. K. Kim and S. S. Yoon, *J. Mater. Chem.*, 2011, **21**, 13640; (j) S. H. Lin, F. I. Wu, H. Y. Tsai, P. Y. Chou, H. H. Chou, C. H. Cheng and R. S. Liu, *J. Mater. Chem.*, 2011, **21**, 8122; (k) H. Park, J. Lee, I. Kang, H. Y. Chu, J. I. Lee, S. K. Kwon and Y. H. Kim, *J. Mater. Chem.*, 2012, **22**, 2695.
- 7 (a) C. C. Wu, Y. T. Lin, K. T. Wong, R. T. Chen and Y. Y. Chien, *Adv. Mater.*, 2004, **16**, 61; (b) Z. P. Silu, X. Zhang, J. Tang, C. S. Lee and S.-T. Lee, *J. Phys. Chem. C.*, 2008, **112**, 2165.
- 8 (a) S. E. Shaheen, G. E. Jabbour, M. M. Morrell, Y. Kawabe, B. Kippelen, N. Peyghambarian, M.-F. Nabor, R. Schlaf, E. A. Mash and N. R. Armstrong, *J. Appl. Phys.*, 1998, **84**, 2324; (b) F. I. Wu, P. I. Shih, M. C. Yuan, C. F. Shu, Z. M. Chung and E. W. G. Diau, *J. Mater. Chem.*, 2005, **15**, 4752; (c) Y. Duan, Y. Zhao, P. Chen, J. Li, S. Liu, F. H and Y. Ma, *Appl. Phys. Lett.*, 2006, **88**, 263503.
- 9 (a) S. Tao, Z. Peng, X. Zhang, P. Wang, C. S. Lee and S. T. Lee, *Adv. Funct. Mater.*, 2005, **15**, 1716; (b) C. Tang, F. Liu, Y. J. Xia, L. H. Xie, A. Wei, S. B. Li, Q. L. Fan and W. J. Huang, *J. Mater. Chem.*, 2006, **16**, 4074; (c) K. C. Wu, P. J. Ku, C. S. Lin, H. T. Shih, F. I. Wu, M. J. Huang, J. J. Lin, I. C. Chen and C. H. Cheng, *Adv. Funct. Mater.*, 2008, **18**, 68.
- 10 (a) A. P. Kulkarni, A. P. Gifford, C. J. Tozola and S. A. Jenekhe, *Appl. Phys. Lett.*, 2005, **86**, 061106; (b) C. J. Tonzola, A. P. Kukarni, A. P. Gifford, W. Kaminsky and S. A. Jenekhe, *Adv. Funct. Mater.*, 2007, **17**, 863; (c) S. J. Lee, J. S. Park, K. J. Yoon, Y. I. Kim, S. H. Jin, S. K. Kang, Y. S. Gal, S. Kang, J. Y. Lww, J. W. Kang, S. H. Lww and H. D. Park, *Adv. Funct. Mater.*, 2008, **18**, 3922.
- 11 (a) H. T. Shih, C. H. Lin, H. S. Shih and H. C. Cheng, *Adv. Mater.*, 2002, **14**, 1409; (b) H. P. Rathnayake, A. Cirpan, P. M. Lahti and F. E. Karasz, *Chem. Mater.*, 2006, **18**, 560; (c) H. P. Rathnayake, A. Cirpan, Z. Delen, P. M. Lahti and F. E. Karasz, *Adv. Funct. Mater.*, 2007, **17**, 115.
- 12 (a) M.A. Baldo, D.F. O' Brien, M.E. Thompson and S. R. Forrest, *Phys. Rev. B*, 1999, **60**, 14422; (b) L. J. Rothberg and A. J. Lovinger, *J. Mater. Res.*, 1996, **11**, 3174.
- 13 S. Difley, D. Beljonne and T.V. Voorhis, *J. Am. Chem. Soc.*, 2008, **130**, 3420.
- 14 (a) M. Segal, M. Singh, K. Rivoire, S. Difley, T. Van Voorhis and M.A. Baldo, *Nat. Mater.*, 2007, **6**, 374; (b) A. Endo, K. Sato, K. Yoshimura, T. Kai, A. Kawada, H. Miyazaki and C. Adachi, *Appl. Phys. Lett.*, 2011, **98**, 083302; (c) K. Goushi, K. Yoshida, K. Sato and C. Adachi, *Nat. Photon.*, 2012, **6**, 253; (d) H. Uoyama, K. Goushi, K. Shizu, H. Nomura and C. Adachi, *Nature*, 2012, **492**, 234.

- 15 Z. R. Grabowski and K. Rotkiewicz, *Chem. Rev.*, 2003, **103**, 3899.
- 16 (a) F. Schneider, E. Lippert and Ber. Bunsen-Ges. *Phys. Chem.*, 1968, **72**, 1155; (b) F. Schneider, E. Lippert and Ber. Bunsen-Ges. *Phys. Chem.*, 1970, **74**, 624; (c) M. Jurczok, T. Custavsson, J.-C. Mialocq and W. Rettig, *Chem. Phys. Lett.*, 2001, **344**, 357; (d) M. Jurczok, P. Plaza, M. M. Martin, Y. H. Meyer and W. Rettig, *Chem. Phys.*, 2000, **253**, 339; (e) N. Asami, T. Takaya, S. Yabumoto, S. Shigeto, H. Hamaguchi and K. Iwata, *J. Phys. Chem. A.*, 2010, **114**, 6351; (f) X. Li, M. Liang, A. Chakraborty, M. Kondo and M. Maroncelli, *J. Phys. Chem. B.*, 2011, **115**, 6592.
- 17 M. sarkar and A. Saman, *Acta Crystallogr. Sect. E.*, 2003, **59**, o1764.
- 18 (a) R. Wortmann, K. Elich, S. Lebus and W. J. Liptay, *Chem. Phys.*, 1991, **95**, 6371; (b) A. Subaric-leitis, C. Monte, A. Roggan, W. Rettig, P. Zimmermann and J. Heinze, *J. Chem. Phys.*, 1990, **93**, 4543; (c) F. C. Grozema, M. Swart, R. W. J. Zijlstra, J. J. Piet, L. D. A. Siebbeles and P. Th. van Duijnen, *J. Am. Chem. Soc.*, 2005, **127**, 11019.
- 19 P. Zhang, W. Dou, Z. Ju, L. Yang, X. Tang, W. Liu and Y. Wu, *Org. Electron.*, 2013, **14**, 915.
- 20 J. Cornil, N. E. Gruhn, D. A. Dos Santos, M. Malagoli, P. A. Lee, S. Barlow, S. Thayumanavan, S. R. Marder, N. R. Armstrong and J. L. Brédas, *J. Phys. Chem. A.*, 2001, **105**, 5206.
- 21 J. S. Reddy, T. Kale, G. Balaji, A. Chandrasekaran and S. Thayumanavan, *J. Phys. Chem. Lett.*, 2011, **2**, 648.
- 22 M. L. Tang and Z. Bao, *Chem. Mater.*, 2011, **23**, 446.
- 23 F. Babudri, G. M. Farinola, F. Naso and R. Ragni, *Chem. Commun.*, 2007, **10**, 1003.
- 24 (a) Z. Li, Z. Wu, B. Jiao, P. Liu, D. Wang and X. Hou, *Chem. Phys. Lett.*, 2012, **527**, 36; (b) Z. Li, Z. Wu, W. Fu, P. Liu, B. Jiao, D. Wang, G. Zhou and X. Hou, *J. Phys. Chem. C.*, 2012, **116**, 20504; (c) Z. Li, B. Jiao, Z. Wu, P. Liu, L. Ma, X. Lei, D. Wang, G. Zhou, H. Hu and X. Hou, *J. Mater. Chem. C.*, 2013, **1**, 2183; (c) Y. Yu, Z. Wu, Z. Li, B. Jiao, L. Li, L. Ma, D. Wang, G. Zhou and X. Hou, *J. Mater. Chem. C.*, 2013, **1**, 8117.
- 25 K. Reichenbacher, H. I. Süss and J. Hulliger, *Chem. Soc. Rev.*, 2005, **34**, 22.
- 26 R. Berger, G. Resnati, P. Metrangolo, E. Weber and J. Hulliger, *Chem. Soc. Rev.*, 2011, **40**, 3496.
- 27 (a) M. A. Kahlou, T. J. Kang and P. F. Barbara, *J. Phys. Chem.*, 1987, **91**, 6452; (b) J. Catalan, C. Diaz, V. Lopez, P. Perez and R. M. Claramunt, *J. Phys. Chem.*, 1996, **100**, 18392.
- 28 (a) C. Adachi, M. E. Thompson, and S. R. Forrest, *IEEE J. Select. Top. Quant. Electron.*, 2002, **8**, 372; (b) M. A. Baldo and S. R. Forrest, *Phys. Rev. B.*, 2000, **62**, 10958.
- 29 M. F. Wu, S. J. Yeh, C. T. Chen, H. Murayama, T. Tsuboi, W. S. Li, I. Chao, S. W. Liu and J.-K. Wang, *Adv. Funct. Mater.*, 2007, **17**, 1887.
- 30 S. J. Su, T. Chiba, T. Takeda and J. Kido, *Adv. Mater.*, 2008, **20**, 2125.
- 31 Y. Li, M. K. Fung, Z. Xie, S. T. Lee, L. S. Hung and J. Shi, *Adv. Mater.*, 2002, **14**, 1317.
- 32 T. Y. Chu and O. K. Song, *Appl. Phys. Lett.*, 2007, **90**, 203512.
- 33 (a) M. S. Kim, B. K. Choi, T. W. Lee, D. Shin, S. K. Kang, J. M. Kim, S. Tamura and T. Noh, *Appl. Phys. Lett.*, 2007, **91**, 251111; (b) Y. Y. Lyu, J. Kwak, O. Kwon, S. H. Lee, D. Kim, C. Lee and K. Char, *Adv. Mater.*, 2008, **20**, 2720; (c) J. Y. Hu, Y. J. Pu, Y. Yamashita, F. Satoh, S. Kawata, H. Katagiri, H. Sasabe and J. Kido, *J. Mater. Chem. C.*, 2013, **1**, 3871.
- 34 T. Tsutsui, E. Aminaka, C. P. Lin and D.-U. Kim, *Philos. Trans. R. Soc. London A*, 1997, **355**, 801.
- 35 (a) C. -G. Zhen, Y. -F. Dai, W. -J. Zeng, Z. Ma, Z. -K. Chen, J. Kieffer, *Adv. Funct. Mater.*, 2011,

- 21, 699; (b) C. Ganzorig, M. Fujihira, *Appl. Phys. Lett.*, 2002, **81**, 3137.
- 36 (a) M. A. Baldo, D. F. O' Brien, M. E. Thompson and S. R. Forrest, *Phys. Rev. B*, 1999, **60**, 14422; (b) L. J. Rothberg and A. J. Lovinger, *J. Mater. Res.*, 1996, **11**, 3174.
- 37 S. M. King, R. Matheson, F. B. Dias and A. P. Monkman, *J. Phys. Chem. B*, 2008, **112**, 8010.
- 38 (a) S. Difley, D. Beljonne, T. V. Voorhis, *J. Am. Chem. Soc.*, 2008, **130**, 3420; (b) M. Mac, A. Danel, A. Michno and R. Królicki, *J. Lumin.*, 2006, **121**, 39; (c) A. S. Lukas, P. J. Bushard, E. A. Weiss and M. R. Wasielewski, *J. Am. Chem. Soc.*, 2003, **125**, 3921.
- 39 (a) Z. E. X. Dance, S. M. Mickley, T. M. Wilson, A. B. Ricks, A. M. Scott, M. A. Ratner and M. R. Wasielewski, *J. Phys. Chem. A*, 2008, **112**, 4194; (b) H. van Willigen, G. Jones II, M. S. Farahat, *J. Phys. Chem.*, 1996, **100**, 3312.

**Table 1** EL performance of blue devices with 3 wt% DPAVBi doped in EML

Device	EML	$\lambda_{\text{max}}^{\text{EL}}$ <sup>a</sup> (nm)	$V_{\text{on}}$ <sup>b</sup> (V)	$L_{\text{max}}$ <sup>c</sup> (cd m <sup>-2</sup> )	$\eta_{\text{ext}}$ <sup>d</sup> (%)	$\eta_{\text{c}}$ <sup>d</sup> (cd A <sup>-1</sup> )	$\eta_{\text{p}}$ <sup>d</sup> (lm W <sup>-1</sup> )	$\eta_{\text{ext}}$ <sup>e</sup> (%)	$\eta_{\text{c}}$ <sup>e</sup> (cd A <sup>-1</sup> )	$\eta_{\text{p}}$ <sup>e</sup> (lm W <sup>-1</sup> )	CIE (x, y) <sup>a</sup>
1A	BAn-(2)-F: DPAVBi	472/49 2	4.1	25065	4.31	8.80	5.79	4.14	8.45	3.09	(0.17,0.33)
2A	BAn-(3)-F: DPAVBi	468/49 2	4.4	25832	4.86	8.67	4.93	4.45	7.93	2.74	(0.16,0.27))
3A	BAn-(4)-F: DPAVBi	468/49 2	3.7	28667	5.43	9.64	6.77	5.24	9.30	3.46	(0.15,0.27)
4A	BAn-(2,4)-F: DPAVBi	468/49 2	4.2	23887	3.56	7.05	4.46	3.35	6.64	2.47	(0.18,0.31)
5A	BAn-(3,4,5)- F: DPAVBi	478/49 2	3.9	17452	4.02	7.98	5.65	3.69	7.29	2.71	(0.17,0.31)

<sup>a</sup> Values collected at 8 V. <sup>b</sup> Turn-on voltage at 1 cd m<sup>-2</sup>. <sup>c</sup> Maximum luminance. <sup>d</sup> Values collected at a peak efficiency. <sup>e</sup> Values collected at a current density of 20 mA cm<sup>-2</sup>.

**Table 2** EL performance of DPAVBi and C545T doped devices

Device	EML	$\Phi_{\text{f}}$ <sup>a</sup>	$L_{\text{max}}$ <sup>b</sup> (cd m <sup>-2</sup> )	$\eta_{\text{ext}}$ <sup>c</sup> (%)	$\lambda_{\text{max}}^{\text{EL}}$ <sup>a</sup> (nm)	FWHM (nm)	CIE (x, y) <sup>d</sup>
1B	BAn-(4)-F: DPAVBi	0.42	26692	5.42	468/492	66	(0.15,0.27)
2B	TBADN: DPAVBi	0.51	22573	3.13	468/492	70	(0.16,0.27))
1C	BAn-(4)-F: C545T	0.48	72829	5.20	504	69	(0.25,0.61)
2C	Alq3: C545T	0.62	58006	3.52	524	60	(0.31,0.64)

<sup>a</sup> Measured in solid doped-EML film (30 nm) on quartz plates by calibrated integrating sphere system. <sup>b</sup> Maximum luminance. <sup>c</sup> Values collected at a peak efficiency. <sup>d</sup> Values collected at 8 V.

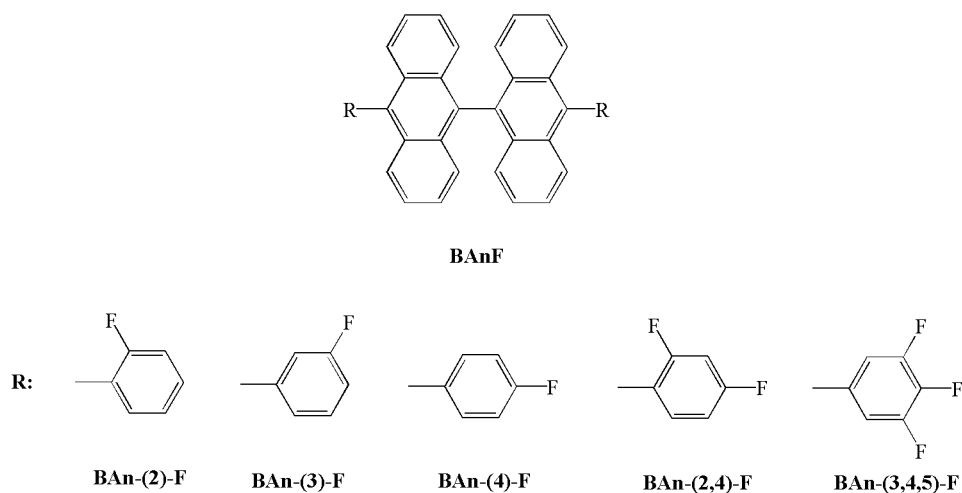


**Fig. 1** Structures of the BAnF compounds.

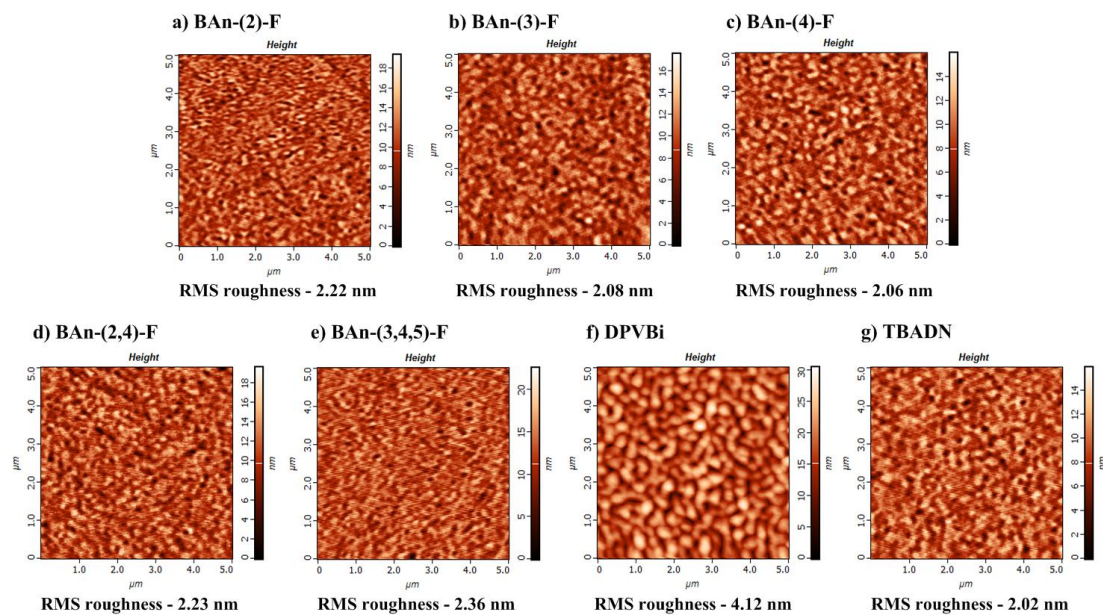


**Fig. 2** The AFM images of the vacuum-deposited films (scan size:  $5 \times 5 \mu\text{m}$ ).

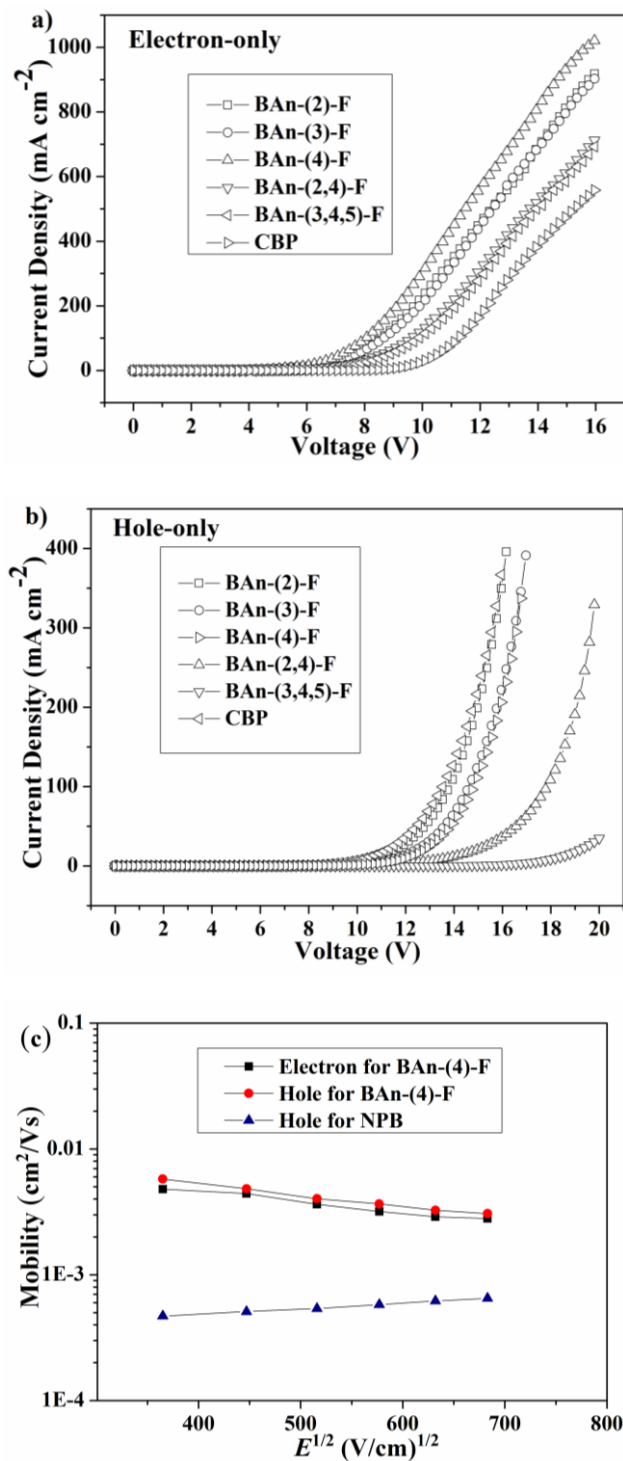


**Fig. 3** (a) Current density–voltage characteristics for the electron-only devices, ITO/LiF (1 nm)/TPBi (10 nm)/BAnF (80 nm)/TPBi (10 nm)/LiF (1 nm)/Al (100 nm). (b) Current density–voltage characteristics for the hole-only devices, ITO/MoO<sub>3</sub> (3 nm)/NPB (10 nm)/BAnF (80 nm)/NPB (10 nm)/MoO<sub>3</sub> (3 nm)/Al (100 nm). (c) Electron and hole mobilities versus  $E^{1/2}$  for BAn-(4)-F, and hole mobilities for NPB.

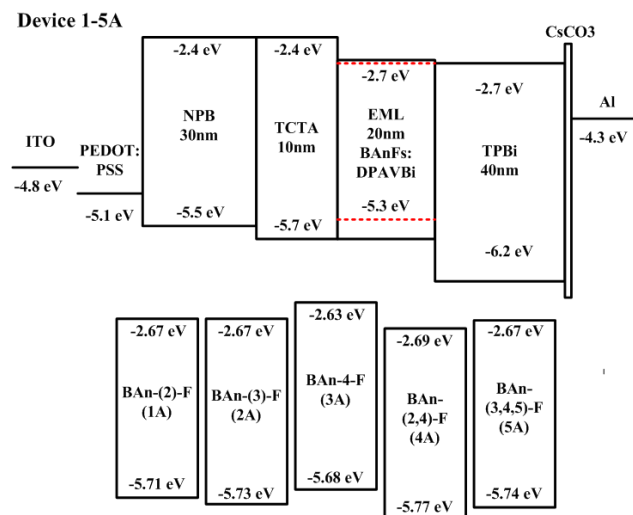


**Fig. 4** Structures of Device1-5A and energy levels of BAnFs.

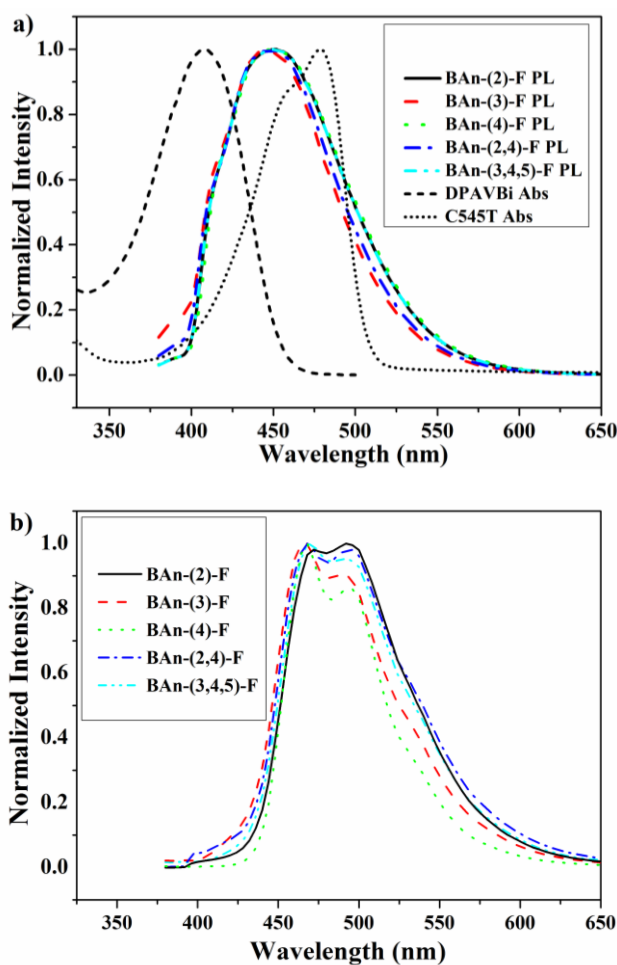


**Fig. 5** (a) PL spectra of BAnFs and absorption spectra of DPAVBi and C545T in CH<sub>2</sub>Cl<sub>2</sub>. (b) EL spectra of DPAVBi-doped devices at 8 V

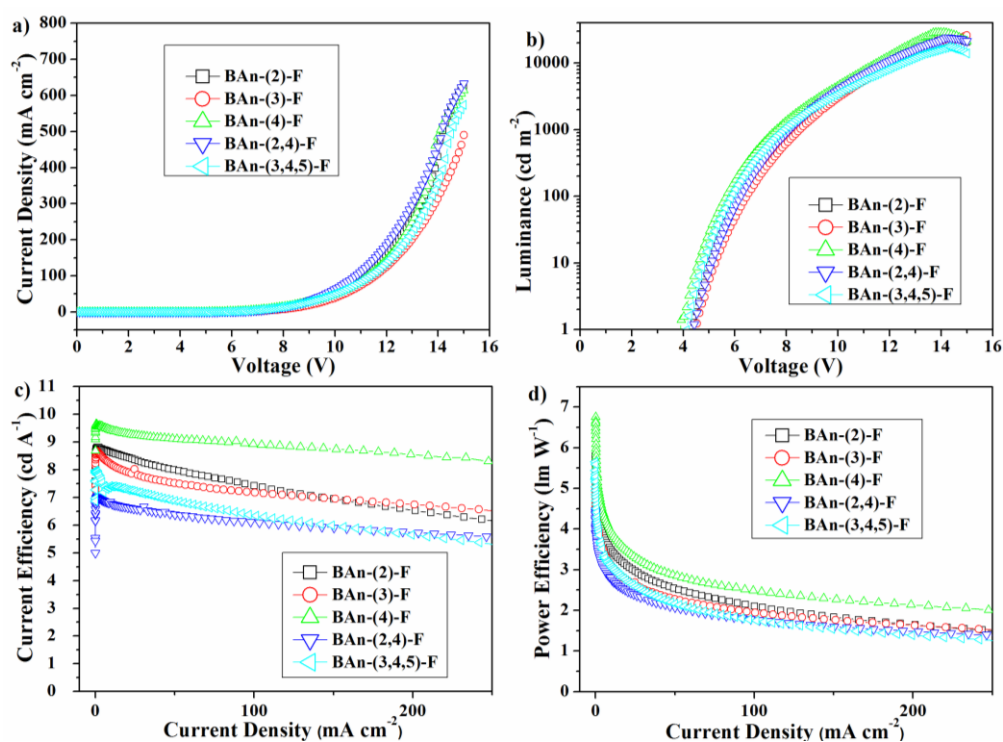


**Fig. 6** (a) Current density–voltage curves. (b) Brightness–voltage curves. (c) Current efficiency–current density curves. (d) Power efficiency–current density curves for DPAVBi-doped devices.

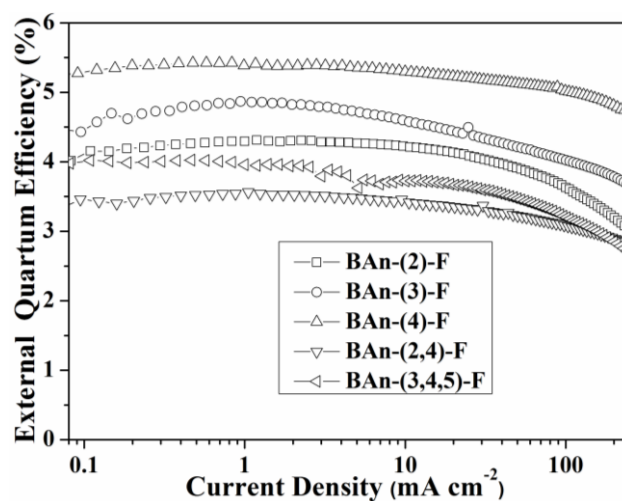


**Fig. 7** External quantum efficiency (EQE) at different current densities for DPAVBi-doped devices.

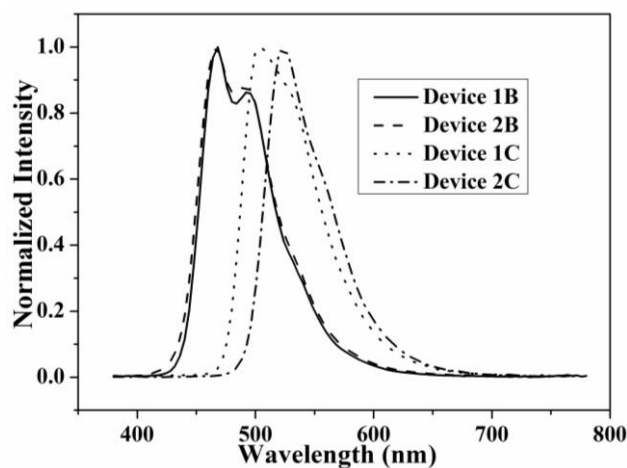


**Fig. 8** EL spectra of DPAVBi and C545T doped devices at 8 V.

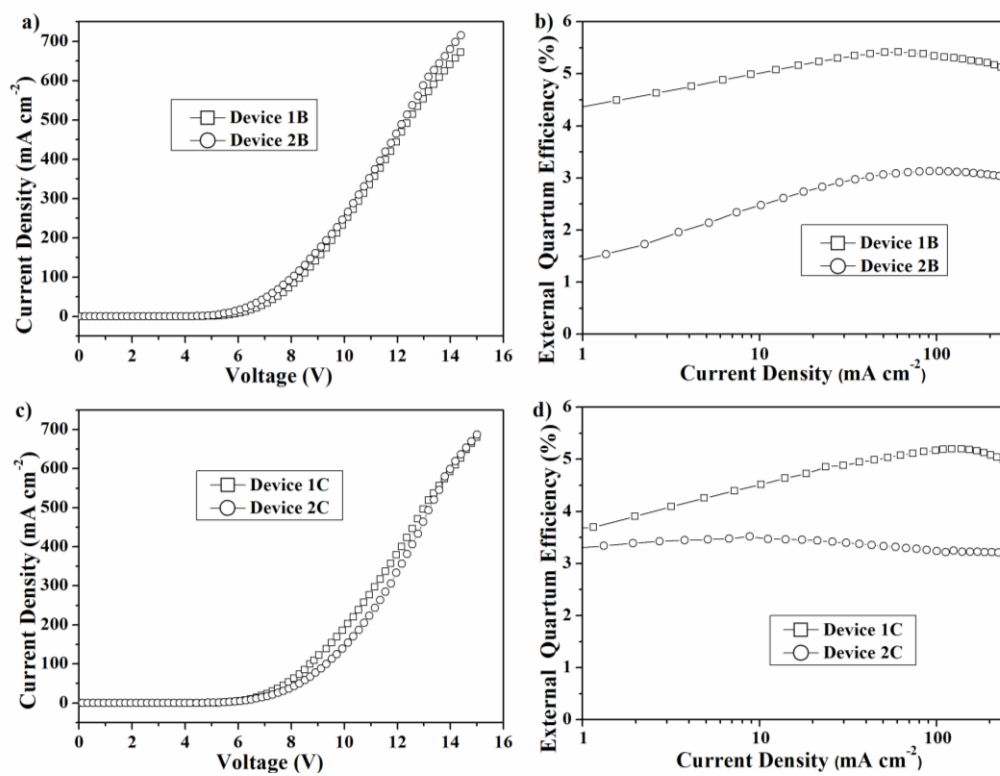


**Fig. 9** (a) Current density–voltage curves of Device 1B and 2B. (b) EQE curves of Device 1B and 2B. (c) Current density–voltage curves of Device 1C and 2C. (d) EQE curves of Device 1C and 2C.

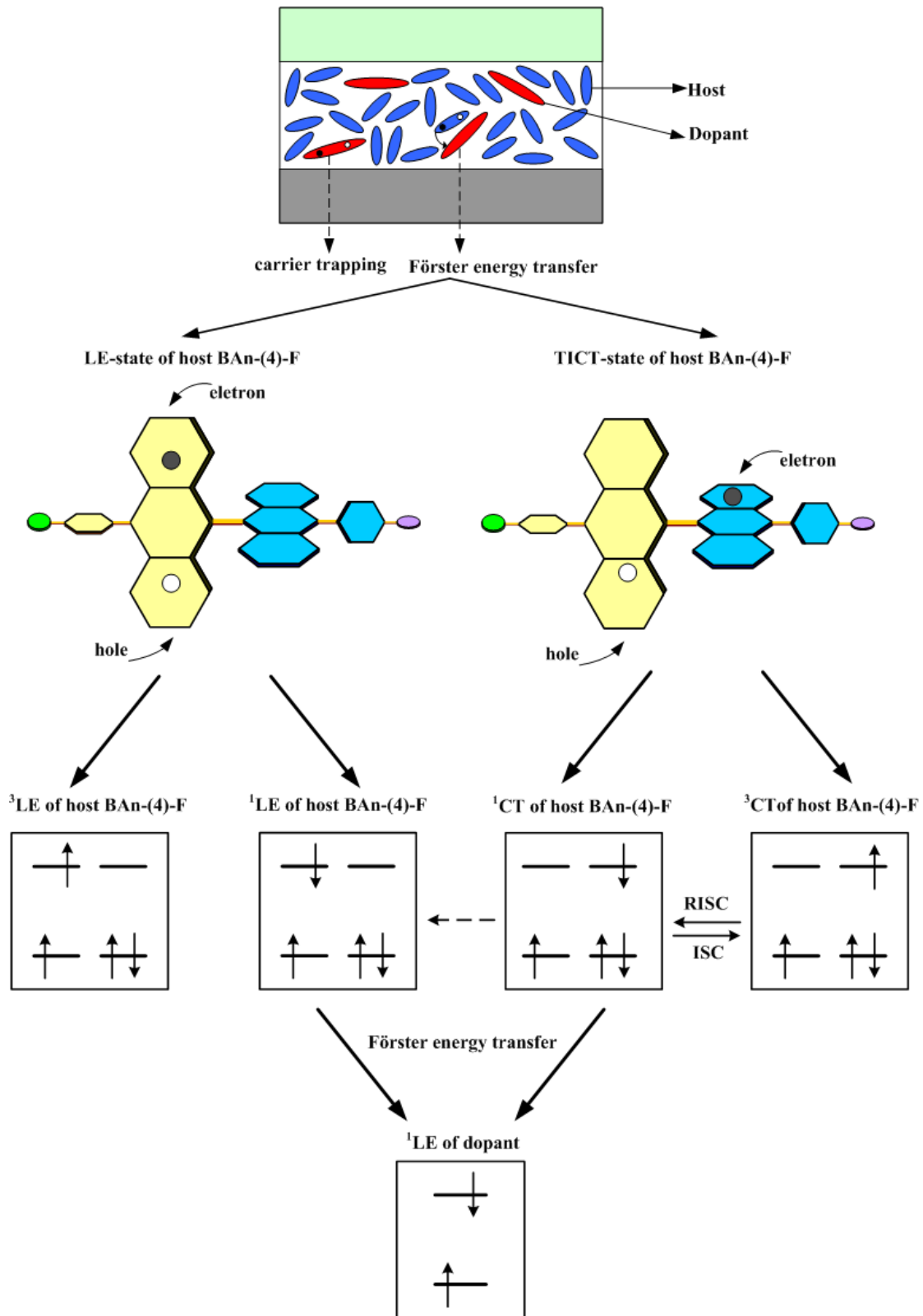


**Fig. 10** Schematic of the formation process of exciton in BAn-(4)-F-based EL device.